A Miniaturized Wideband Wilkinson Power Divider for IoT Sub-GHz Applications

Shaimaa A. Osman[1, 2, *], Mohamed S. El-Gendy[2],
Hadia M. Elhennawy[1], and Esmat A. F. Abdallah[2]

Abstract—This paper presents a single stage 2-way Wilkinson Power Divider (WPD) suitable for Internet of Things (IoT) low frequency applications in the band from 200 MHz to 1 GHz. It is realized using a meandered line, and an open shunt stub matching network is added to get a compact structure. Moreover, a Vertical Periodic Defected Ground Structure (VPDGS) is added below each arm in order to improve the performance at the center frequency without adding extra length to the divider. The size of the proposed power divider is $30 \times 15.3\,\text{mm}^2$ ($0.082\lambda_g \times 0.041\lambda_g$). The fabricated power divider achieves a fractional bandwidth of 107%, an input return loss of better than 10 dB, an output return loss of 20 dB, an isolation of better than 10 dB, and maximum exceeded insertion loss of 0.9 dB. The proposed compact power divider is implemented on Rogers RT/Duroid 5880 with thickness 0.254 mm in order to bend on any conformal surface.

1. INTRODUCTION

Internet of Things (IoT) is a revolution concept of connecting physical smart objects, called Things, that embed electronics, software, and sensors within a network to collect and exchange data with other networks. IoT is considered as a network of networks that helps in improving the quality of the daily life. As with any new technology concept, IoT encouraged the research in multidiscipline such as agriculture automation, smart homes, wildlife/fire monitoring, telemedicine, and healthcare [1]. Telemedicine and healthcare monitoring systems may include Smart Wireless Capsule Endoscopy (S-WCE) transmitter, on-body transmitter, and off-body receiver. As the transmitter is portable, a receiver with high gain and interference immunity is required. Antenna array for the receiver is a good candidate to improve the communication reliability between the transmitter and receiver.

Power divider (PD) is a fundamental passive circuit usually used as a feeding network for antennas array [2–7]. It can be not only employed with antenna arrays but also used in power amplifiers [8–11] and mixers [12–14]. Power dividers and combiners can be classified as a circulator, T-junction [15], and Wilkinson Power Divider (WPD) [16]. The last one is usually recommended for its matched ports, lossless and isolated output ports using a resistor, although the conventional WPD suffers from a very narrow bandwidth.

In order to recover this, different bandwidth (BW) broadening techniques can be used such as using multi-section of WPD. For instance, [17] used a quarter-wavelength binomial three-section WPD to get an input return loss Fractional Bandwidth (FBW) of 110%. A three-section WPD with two hemi-circles Defected Ground Structures (DGS) is discussed in [18]. Another three-section meandered WPD is introduced in [19], where four butterfly combs DGSs are installed on each arm of the WPD to achieve an FBW of 133%. Another broadening technique is to replace each uniform quarter wavelength arm with a taper line. For example, [20] replaced a quarter wavelength transmission line with a Klopfenstein

* Corresponding author: Shaimaa Abdelaziz Mahmoud Osman (shaimaa.osman@eri.sci.eg).
[1] Electronics and Electrical Communication Engineering Department, Ain Shams University, Cairo, A.R.E. [2] Microstrip Circuits Department, Electronics Research Institute, Cairo, A.R.E.

tapered line and installed seven isolation resistors on the line to maintain a wide return loss bandwidth. Ref. [21] introduced a multilayer wideband PD, where a patch on the top layer (input port) was coupled through a slot on the middle layer to two half-patches (output ports) on the bottom layer. A wide tunable division ratio PD was proposed in [22] with two varactors for controllability. A quad band WPD was presented in [23], where an extended composite right left handed (E-CRLH) metamaterial replaced each arm of the WPD to attain a wide BW ratio of $> 70\%$ for the first two bands. Ref. [24] discussed a single section WPD loaded with an isolation network consisting of coupled lines, a quarter wavelength transmission line, and a resistor. Ref. [25] introduced a meandered single stage WPD to achieve a compact size. Adding an open or short stub network to the WPD arms is a very common technique in broadening the BW without adding an extra length for the PD. For instance, a single stub network was used in [26–29], double stubs in [30, 31], and triple stubs in [32]. Furthermore, different shapes of stubs can be used other than the conventional rectangular stub like radial stub [33] and triangle stub [34]. A PD with a triple mode resonator with an open shunt stub and parallel coupled lines replacing the quarter wavelength arm is presented in [35]. Ref. [36] replaced the conventional $\lambda/4$ transmission line with a T-shaped transmission line to obtain a miniaturized splitter and coupler structures. Ref. [37] replaced the conventional microstrip line with its equivalent T-section to design hybrid couplers with a 50% size reduction.

One of the common techniques to improve the circuit performance is using a DGS. It is an etching in the ground plane that changes the inductance and capacitance of the Transmission Line (TL), hence shifting the center frequency without changing the total area of the design. It can take any geometry such as simple square, dumbbell, spiral head, H-shape, interdigital, etc. [38]. More complicated structures can be implemented using periodic repetition of simple dumbbell DGS such as Vertical Periodic DGS (VPDGS) and Horizontal Periodic DGS (HPDGS) which achieve a 44.4% and 38.5 size reduction, respectively as in [39]. Ref. [40] discussed a three-sections WPD with a series resistor-capacitor isolation network and DGS with overall length of quarter wavelength and broadband characteristics.

In this paper, a wideband power divider is introduced for IoT sub-GHz applications. The proposed design is analyzed, designed, then implemented in a miniaturized size. The rest of the paper is organized as follows. Section 2 discusses the structure of the proposed power divider. Section 3 explains the analytical solution and the equivalent circuit for the proposed design. Fabrication, measurements, results, and comparative study are reported in Section 4. Finally, Section 5 concludes the paper.

2. STRUCTURE OF THE PROPOSED POWER DIVIDER

Figure 1 shows the proposed power divider, where the power divider is meandered, an open shunt stub network installed on each arm, and each arm has a VPDGS in the ground plane in order to achieve a compact size and broaden bandwidth. The performance at the center frequency is adjusted without adding extra lengths to the proposed PD. Table 1 summarizes the final dimensions of the proposed PD. In the following section, the design and analysis procedures that lead to the proposed design are elaborated.

Table 1. Final dimensions for the proposed power divider (units in mm).

Feed line		PD arm			Stub				VPDGS					
L_f	W_f	L_a	W_a	S_a	L_{s1}	L_{s2}	W_s	S_s	L_d	W_d	W_{d2}	S_d	O_{d1}	O_{d2}
4.4	0.8	12	0.45	0.45	1.6	9	0.5	2.6	12	0.45	0.2	3.95	0.25	0.1

## 3. DESIGN PROCEDURES AND ANALYSIS

3.1. Analytical Solution

For the conventional transmission line WPD shown in Fig. 2(a), apply the even odd mode analysis [41] to get the characteristic impedance of each arm $Z_t = \sqrt{2}Z_o$, $R = 2Z_o$, and each arm has an electrical
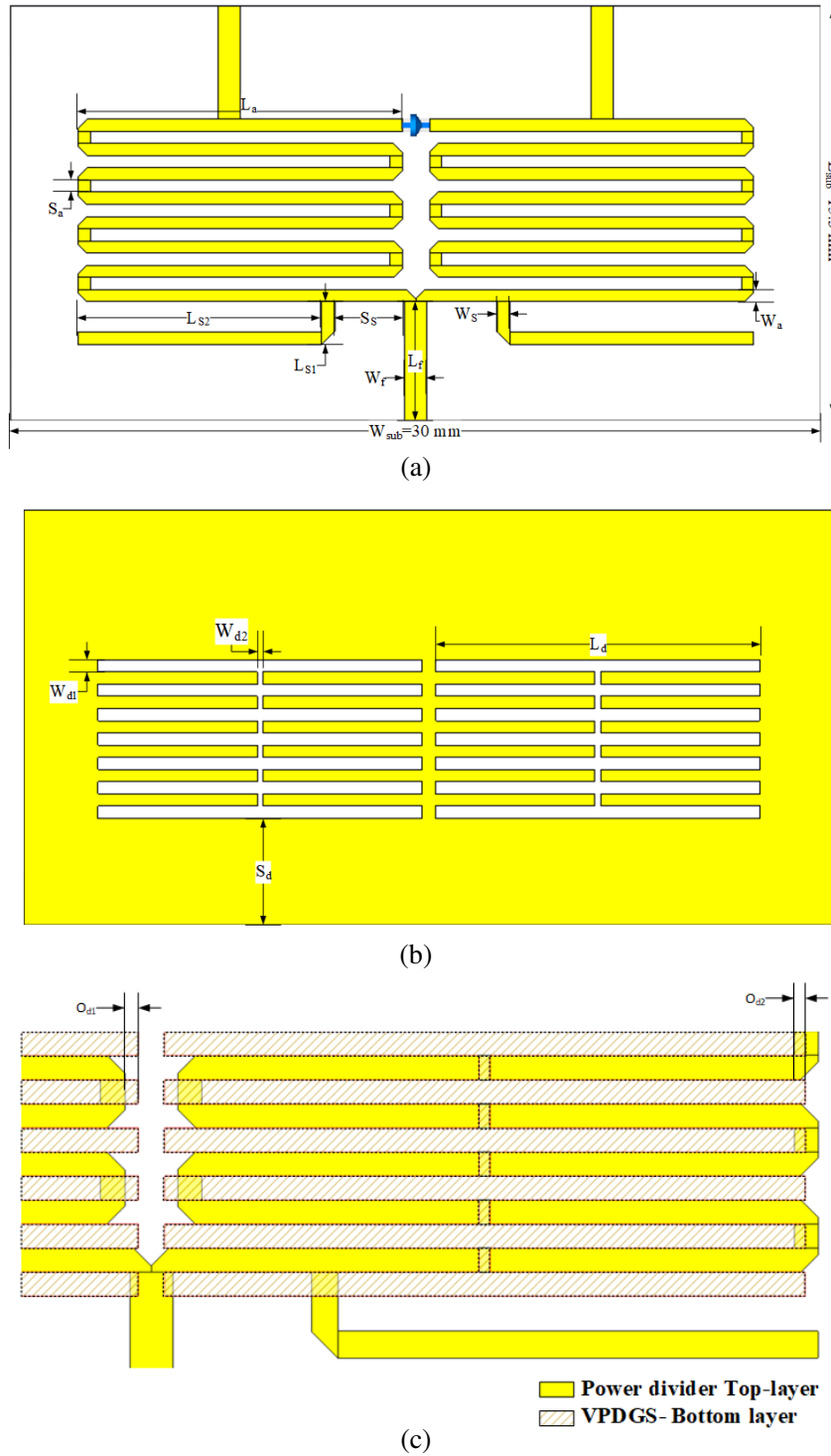
Figure 1. Schematic diagram of the proposed wideband PD, (a) front-side view and (b) back-side view, and (c) enlarged view of the DGS position beneath the power divider.

length of $\varphi = 90°$. An open stub is loaded on each arm for miniaturization purposes as shown in Fig. 2(b). Following the procedures provided in [29], where the input and output TLs are balanced at 50 ohms; therefore, their effect is neutralized and can be deleted from the analysis. In order to find the equations for the characteristic impedance of the TL and the stub (Z_1 and Z_s) of the proposed PD
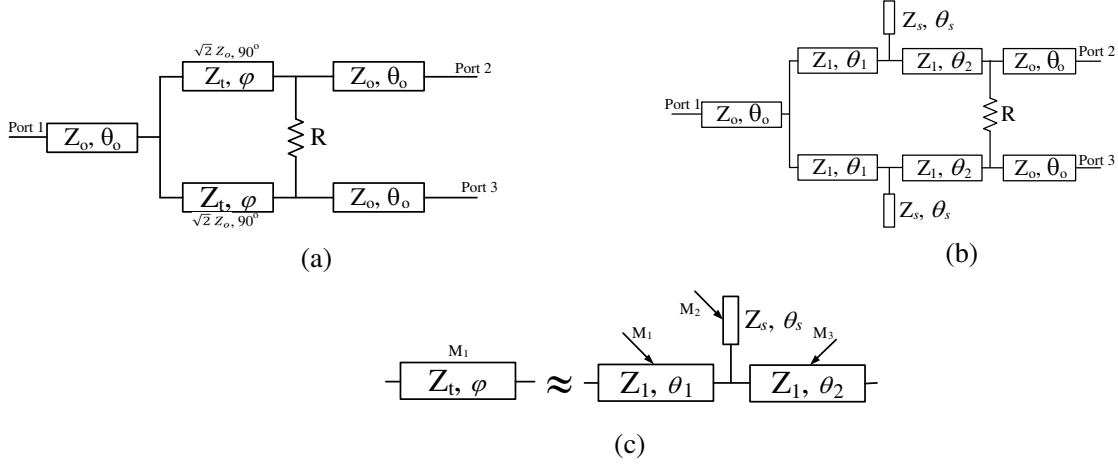
Figure 2. Schematic diagram for the transmission line model of the proposed PD, (a) simplified PD with fixed input and output ports, (b) complete power divider with open stub, and (c) Matrices equivalency between the simplified design and the complete one.

relative to the conventional WPD's parameters, an $ABCD$ matrix analysis [42] is carried out. This is done by replacing each element with its equivalent matrix as shown in Fig. 2(c) where

$$M_t = M_1 M_2 M_3 \tag{1}$$

$$
\begin{bmatrix}
\cos \varphi & jZ_t \sin \varphi \\
j\dfrac{\sin \varphi}{Z_t} & \cos \varphi
\end{bmatrix}
=
\begin{bmatrix}
\cos \theta_1 & jZ_1 \sin \theta_1 \\
j\dfrac{\sin \theta_1}{Z_1} & \cos \theta_1
\end{bmatrix}
\begin{bmatrix}
1 & 0 \\
j\dfrac{\tan \theta_s}{Z_s} & 1
\end{bmatrix}
\begin{bmatrix}
\cos \theta_2 & jZ_1 \sin \theta_2 \\
j\dfrac{\sin \theta_2}{Z_1} & \cos \theta_2
\end{bmatrix}.
\tag{2}
$$

Solve for Z_1 and Z_s, to get:

$$Z_1 = \sqrt{2} Z_o \frac{\cos \theta_2 - \cos \varphi \cos \theta_1}{\sin \varphi \sin \theta_1} \tag{3}$$

$$Z_s = \tan \theta_s \frac{Z_1 \sin \theta_1 \cos \theta_2}{\cos (\theta_1 + \theta_2) - \cos \varphi} \tag{4}$$

The next step is to tune θ_1, θ_2, and θ_s in Agilent ADS to obtain a satisfactory initial wide bandwidth and a compact electrical length ($\theta_1 + \theta_2 < 90°$) that will be modified further when the design is implemented in microstrip (MS) technology where the substrate losses take effect. Fig. 3 shows the performance of the conventional WPD versus the proposed power divider. It can be observed that the center frequency is shifted down. This will be improved in the microstrip realization. The initial physical dimensions of the proposed design on a Rogers RT/Duroid 5880 substrate ($\varepsilon_r = 2.2$, $h = 0.254$ mm, $\tan \delta = 0.0009$) are obtained from Agilent LineCalc and summarized in Table 2 along with the initial electrical dimensions.

Table 2. Initial electrical and physical dimensions of the proposed PD.

Electrical Dimensions							Physical Dimensions (in mm)						
Z_o	θ_o	θ_1	θ_2	θ_s	Z_1	Z_s	W_o	L_o	W_1	L_1	L_2	W_s	L_s
$50\,\Omega$	$5°$	$12.4°$	$76°$	$10°$	$79.66\,\Omega$	$26.13\,\Omega$	0.34	5.1	0.34	12.9	79.2	1.9	9.88

The initial physical dimensions are further modified in the microstrip technology to adjust the performance at the center frequency which lead to the final dimensions shown in Fig. 1 and Table 1. The microstrip evolution steps are as follows: (1) Meandering the arms of the PD, Meander_only. (2) Adding an open stub to each meandered arm, Meander_Stub. (3) Defecting the ground beneath the
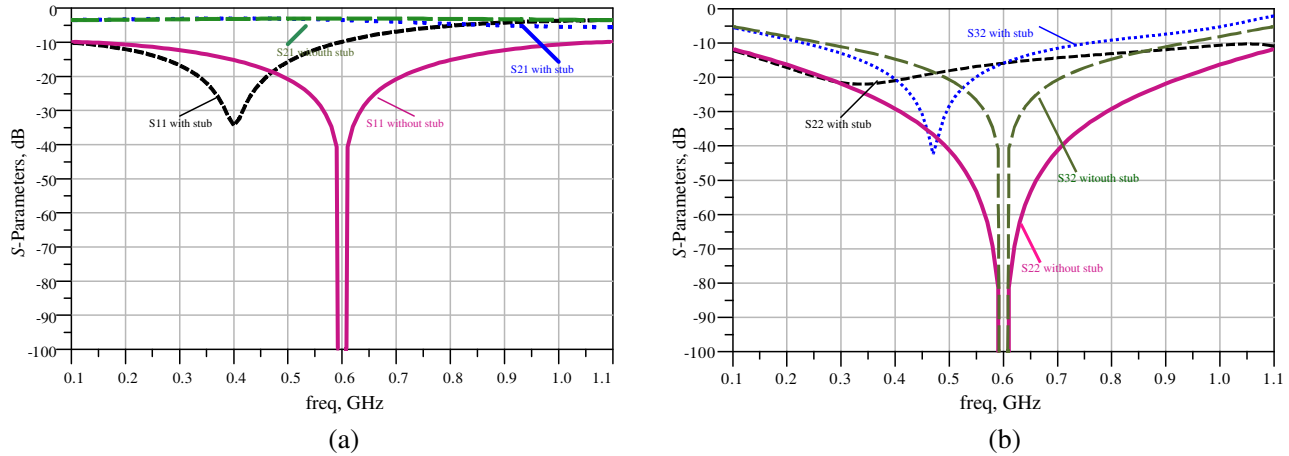
Figure 3. Performance of the conventional WPD vs. the proposed TL PD, (a) insertion loss and input return loss, (b) output return loss and isolation.

meandered PD with the stub, Meander_Stub_DGS. Meandering the PD gives the main miniaturization effect (reducing the vertical length of each arm from around 79 mm without meandering to only 6.5 mm after meandering), where the center frequency for the input return loss is at 758 MHz. Instead of adding extra length for further shifting down the operating frequency, a stub is added which helped in moving down the frequency to 617 MHz. The final step is just for fine tuning the frequency by disturbing the current distribution in the ground plane by defecting it. To get the benefit of the ground space without adding extra length, the VPDGS lowered the operating frequency from 617 to 597 MHz.

The DGS used is based on the simplest form of DGS, which is a dumbbell DGS beneath the microstrip line. Since each arm is a meandered line, underneath each horizontal segment of the line, a dumbbell is inserted. The dumbbells are combined to create the periodic structure depicted in Fig. 1(c). After that, with a simple tuning of the length of the defect and vertical gap, the S-parameters are adjusted near the center frequency. The S-parameters for the different evolution steps are depicted in Fig. 4.

3.2. Equivalent Circuit

The proposed power divider design approach starts from the output of the even-odd mode analysis ($Z_t = \sqrt{2}Z_o$, $R = 2Z_o$). The second step is to apply the $ABCD$ matrix analytical method to find the equivalency between the simplified and complete forms of the PD with the open stub. The third step is carrying out a parametric study using an ADS circuit simulator to find the electrical length ratios for the T-section. The next step is the implementation of the meandered PD with the open stub in microstrip technology with the aid of the CST full-wave simulator. Since the S-parameters are not well adjusted at the center frequency, a modification is needed either by adding an extra length to the meandered PD at the expense of the area or by modifying the ground. Defecting the ground saves the area; therefore, it is chosen. During the previous steps, the analytical solution and parametric study, DGS is not considered to reduce the complexity. Consequently, the equivalent circuit model is introduced to get a physical insight of the defected structure that gives comparable results with that of CST. The power divider can be presented as a π-network or T-network [43] of inductance L_p and capacitance C_p. Then the open stub equivalent of series L_s and C_s is added. Finally, the DGS equivalent is added. DGS can be presented as only parallel LC circuit, parallel RLC circuit, π-network, and a quasi-static equivalent circuit [38]. Here, LC circuit is chosen for its simplicity to represent the DGS, L_d, and C_d. Fig. 5 shows the equivalent circuit for the proposed PD. The steps carried out to find the equivalent circuit are summarized in the flowchart shown in Fig. 6.

It starts with finding an equivalent lumped circuit for the proposed MS meandered PD with the open stub only. Once the performance for both designs are nearly the same, an initial DGS equivalent circuit is added and tuned till it meets the performance of the final MS design with DGS. The final lumped elements values are summarized in Table 3. The performance for both MS and lumped designs
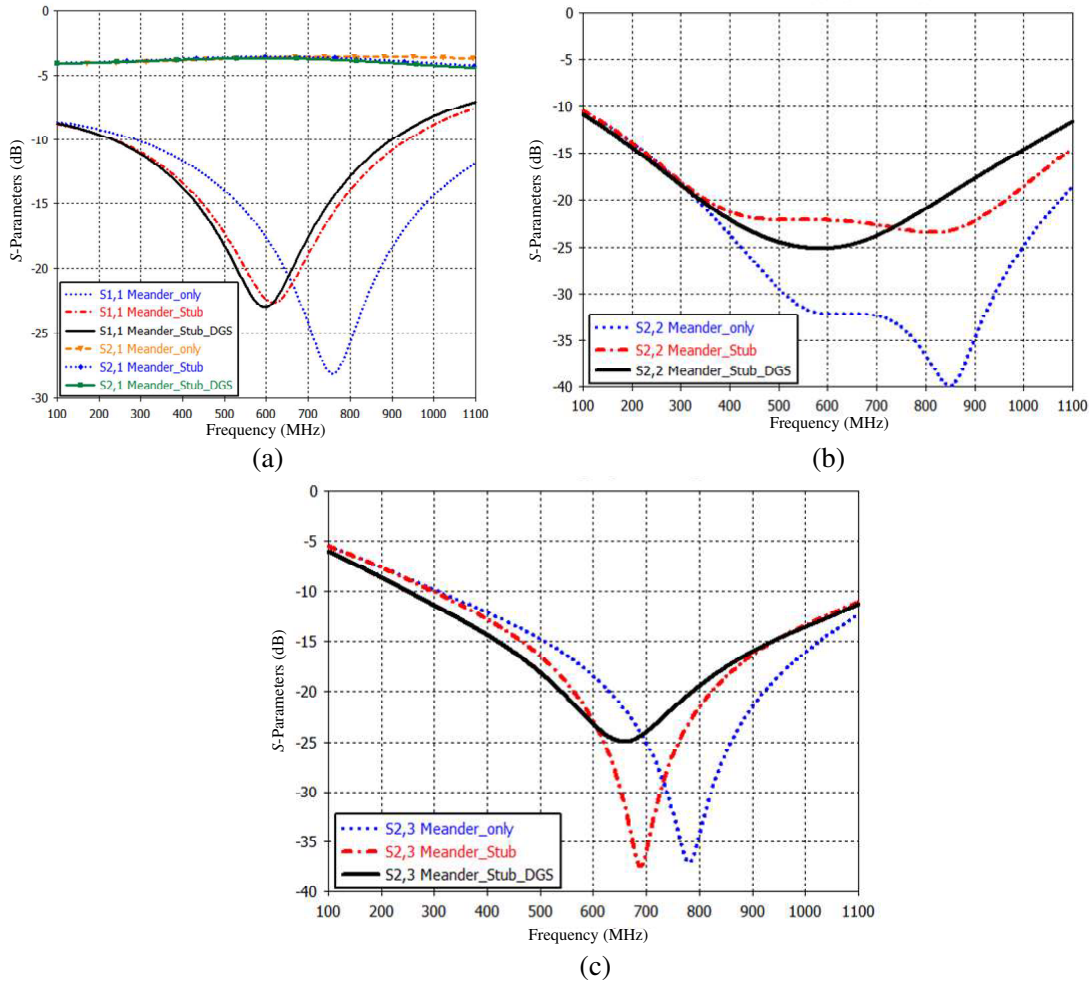
Figure 4. *S*-parameters of the proposed PD at different evolution steps, (a) insertion loss and input return loss, (b) output return loss, and (c) isolation.
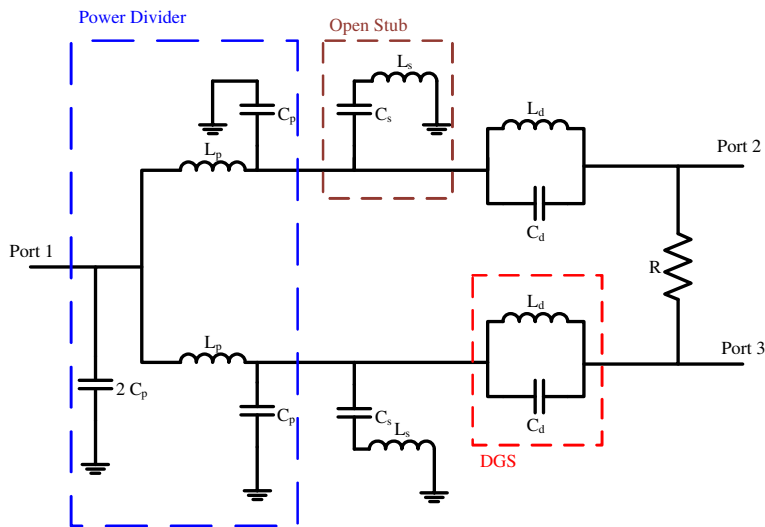
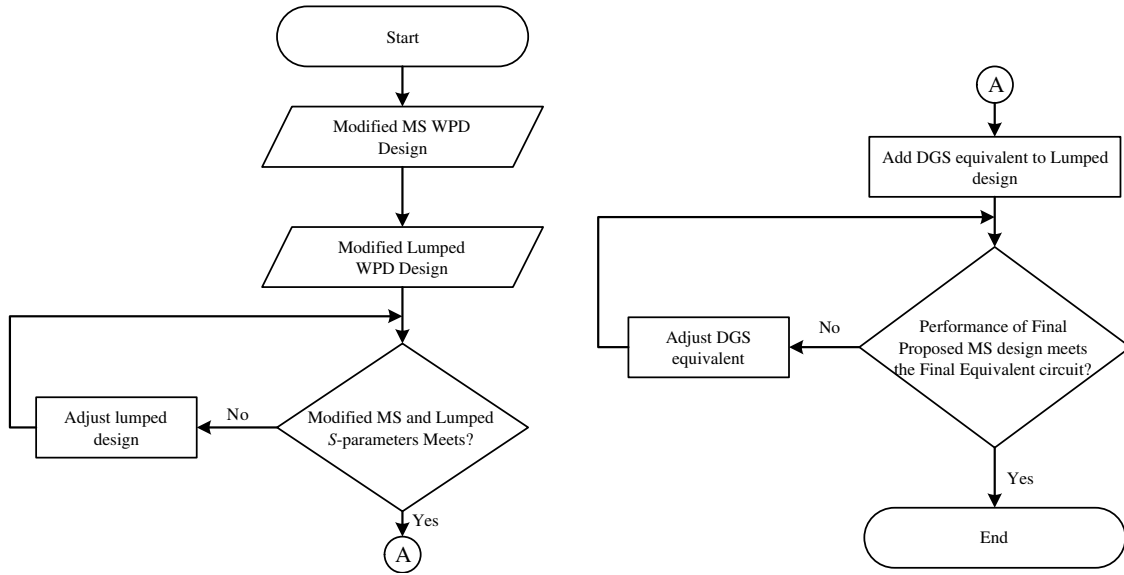**Figure 5.** Lumped-elements model of the proposed PD.

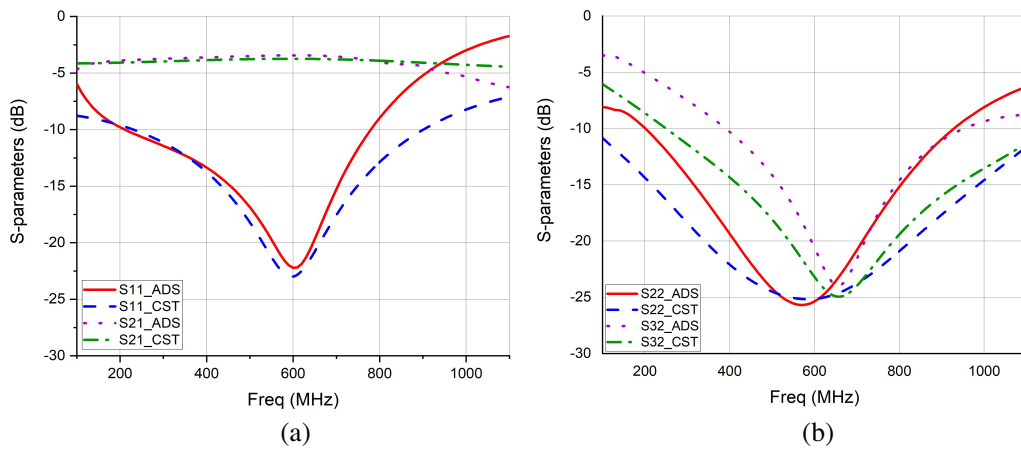**Figure 6.** A flowchart summarizing the procedures to find the equivalent model for the proposed PD.

Figure 7. Performance of the microstrip design vs lumped element model, (a) insertion loss and input return loss, and (b) output return loss and isolation.

**Table 3.** Equivalent circuit values for the proposed PD.

π-Power Divider		Open Stub		DGS		
C_p pF	L_p nH	C_s pF	L_s nH	C_d pF	L_d nH	$R\,\Omega$
2.85	19	106	130	96	98	100

(simulated in CST and ADS simulators, respectively) are shown in Fig. 7, where one finds that the performance at the center frequency is almost identical with some discrepancies at the upper edge of the frequency band.

4. RESULTS AND MEASUREMENTS

The proposed power divider is fabricated on Rogers RT/Duroid 5880 with ε_r of 2.2, loss tangent of 0.0009, and substrate thickness of 0.254 mm using photolithographic technique. The vertical length of

each arm after meandering is only 6.5 mm as opposed to around 79 mm without meandering, representing an approximate 91% reduction in the vertical length. The total size including the input and output ports is 30 mm × 15.3 mm as shown in Fig. 8. The measurements are carried out using Rohde & Schwarz ZVA67 vector network analyzer. Fig. 9 shows that there is a good agreement between the simulation results from CST and the measured ones, where for a fractional bandwidth of 107% (from 290 MHz to 936 MHz) the exceeded insertion loss is 0.9 dB; the input return loss is better than 10 dB; the output return loss and isolation are better than 20 dB and −10 dB, respectively. These S-parameters values validate the proposed PD design. A comparative study for the proposed PD with other published wideband PDs is shown in Table 4, where all references in comparison are modified WPDs with wide bandwidth. As can be observed, the proposed PD achieved a wideband with a compact size, only a single stage of WPD, and a single lumped element.
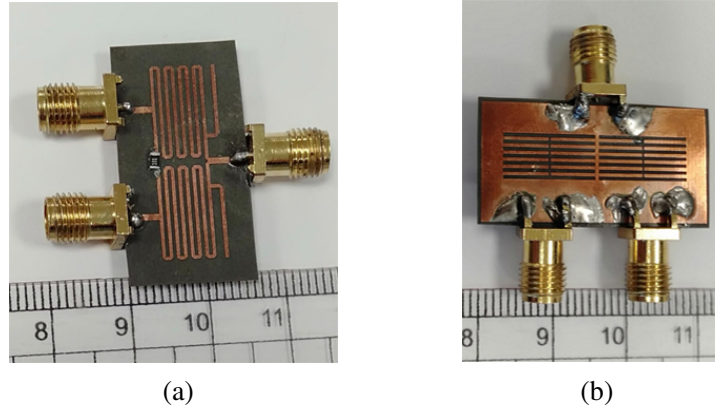
Figure 8. Fabricated 2-way power divider, (a) front-side and (b) ground side.

Table 4. A comparison between the proposed design and other published wideband PDs.

	This work	[24]	[25]	[35]	[40]	[44]
F_o (MHz)	600	1000	433	2500	500	2200
FBW %	107.7	107	66.7*	78	101	150
Size $\lambda_g \times \lambda_g$	0.082×0.041	0.36×0.33	$0.085 \times 0.071^*$	0.74×0.31	$0.25 \times -$	$1.22^* \times -$
(mm × mm)	(30×15.3)	(65.8×59)	(40.1×33.5)	$(- \times -)$	$(107 \times -)$	$(70 \times -)$
S_{11} (dB)	−10	−10	−14*	−10	−20	−10
Exceeded S_{21} (dB)	−0.9	−0.9	0.25	−0.7	−0.45	−2
S_{22} (dB)	−20	−16	25.58	−10	−20	−10
S_{32} (dB)	−10	−24	−15	−17.5	−20	−10
Substrate	$\varepsilon_r = 2.2$ $h = 0.254$	$\varepsilon_r = 3.55$ $h = 1.524$	$\varepsilon_r = 4.4$ $h = 1.6$	$\varepsilon_r = 3.66$ $h = 1.524$	$\varepsilon_r = 4.5$ $h = 0.6$	$\varepsilon_r = 10.2$ $h = 0.635$
Design Methodology	Single-section Meandered WPD with open stub and DGS	Single-section WPD with isolation network of coupled lines, $\lambda/4$ TL and Resistor	Single-section Meandered WPD	Single-section parallel coupled line WPD with single stub	Three-sections WPD with RC isolation circuit and DGS	Five-sections WPD with extra RC circuit at the output port
* The value is not given explicitly, it is deduced from the given results.						
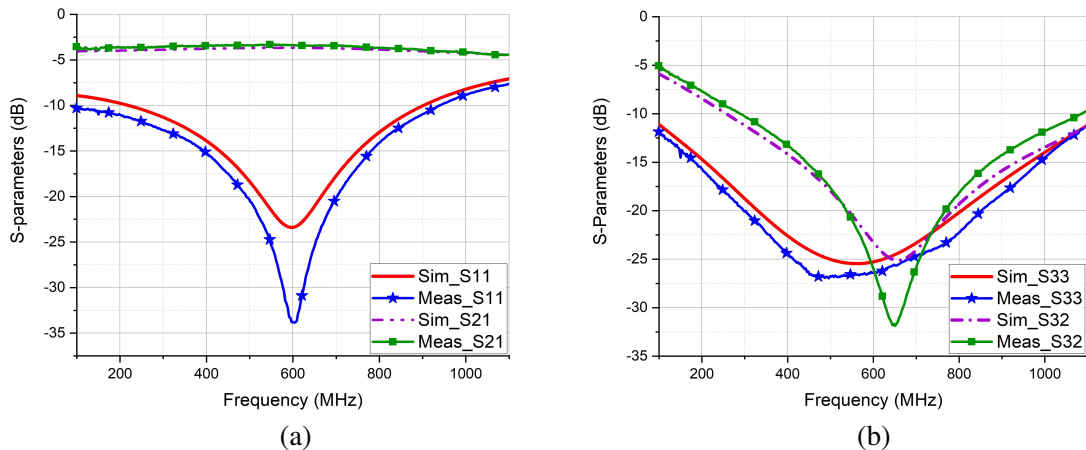
Figure 9. Simulation vs Measurement of the proposed PD.

5. CONCLUSIONS

In this paper, a miniaturized wideband 2-way power divider for IoT applications is proposed. The proposed design is a single-section meandered line WPD with an open stub network and a DGS in order to improve the bandwidth, matching, and isolation at the whole band. An analytical solution along with an equivalent circuit for the proposed design is discussed. The proposed PD is fabricated and measured. A good agreement between simulation and measurement validates the power divider. Moreover, the fabricated PD achieves a fractional bandwidth of 107% and miniaturized size of 30 mm × 15.3 mm. Furthermore, the proposed PD is implemented on a thin substrate of thickness 0.254 mm in order to fit for conformal applications.

REFERENCES

1. Misra, G., V. Kumar, A. Agarwal, and K. Agarwal, "Internet of things (IoT) — A technological analysis and survey on vision, concepts, challenges, innovation directions, technologies, and applications (an upcoming or future generation computer communication system technology)," *American Journal of Electrical and Electronic Engineering*, Vol. 4, 23–32, 2016.

2. Jin, H., G. Q. Luo, W. Wang, W. Che, and K.-S. Chin, "Integration design of millimeter-wave filtering patch antenna array with SIW four-way anti-phase filtering power divider," *IEEE Access*, Vol. 7, 49804–49812, 2019.

3. Reese, R., M. Jost, M. Nickel, E. Polat, R. Jakoby, and H. Maune, "A fully dielectric lightweight antenna array using a multimode interference power divider at W-band," *IEEE Antennas and Wireless Propagation Letters*, Vol. 16, 3236–3239, 2017.

4. Xiao, B., H. Yao, M. Li, J.-S. Hong, and K. L. Yeung, "Flexible wideband microstrip-slotline-microstrip power divider and its application to antenna array," *IEEE Access*, Vol. 7, 143973–143979, 2019.

5. Shanmugam Bhaskar, V. and E. L. Tan, "Power divider with wideband harmonic suppression for center-fed antenna arrays," *Microwave and Optical Technology Letters*, Vol. 63, 3008–3014, 2021.

6. Ali, M., A. O. Watanabe, T.-H. Lin, D. Okamoto, M. R. Pulugurtha, M. M. Tentzeris, et al., "Package-integrated, wideband power dividing networks and antenna arrays for 28-GHz 5G new radio bands," *IEEE Transactions on Components, Packaging and Manufacturing Technology*, Vol. 10, 1515–1523, 2020.

7. Mohammadi, P., A. Piroutiniya, and M. H. Rasekhmanesh, "A novel compact feeding network for array antenna," *Progress In Electromagnetics Research Letters*, Vol. 59, 101–107, 2016.

8. Feng, W., Y. Shi, X. Y. Zhou, X. Shen, and W. Che, "A bandpass push–pull high power amplifier based on SIW filtering balun power divider," *IEEE Transactions on Plasma Science*, Vol. 47, 4281–4286, 2019.

9. Kim, K. and C. Nguyen, "A V-band power amplifier with integrated Wilkinson power dividers-combiners and transformers in 0.18-μm SiGe BiCMOS," *IEEE Transactions on Circuits and Systems II: Express Briefs*, Vol. 66, 337–341, 2018.

10. Nouri, M. E., S. Roshani, M. H. Mozaffari, and A. Nosratpour, "Design of high-efficiency compact Doherty power amplifier with harmonics suppression and wide operation frequency band," *AEU — International Journal of Electronics and Communications*, Vol. 118, 153168, May 1, 2020.

11. Qi, X. and F. Xiao, "Filtering Doherty power amplifier," *IET Microwaves, Antennas & Propagation*, Vol. 14, 1074–1078, 2020.

12. Zhang, L., X. Tong, J. A. Han, and X. Cheng, "A 45-61 GHz monolithic microwave integrated circuit subharmonic mixer incorporating dual-band power divider," *Microwave and Optical Technology Letters*, Vol. 62, 2851–2856, 2020.

13. Chang, Y.-T. and H.-C. Lu, "A V-band ultra low power sub-harmonic I/Q down-conversion mixer using current re-used technique," *IEEE Transactions on Circuits and Systems II: Express Briefs*, Vol. 67, 2893–2897, 2020.

14. Yoon, K. C. and K. G. Kim, "Miniaturization of a single-ended mixer using T-shaped Wilkinson power combiner for medical wireless communication applications," *Microwave and Optical Technology Letters*, Vol. 61, 1977–1982, 2019.

15. Piroutiniya, A. and P. Mohammadi, "The substrate integrated waveguide T-junction power divider with arbitrary power dividing ratio," *The Applied Computational Electromagnetics Society Journal (ACES)*, 428–433, 2016.

16. Pozar, D. M., *Microwave Engineering*, 4th Edition, Wiley, 2011.

17. Mishra, B., A. Rahman, S. Shaw, M. Mohd, S. Mondal, and P. P. Sarkar, "Design of an ultra-wideband Wilkinson power divider," *2014 First International Conference on Automation, Control, Energy and Systems (ACES)*, 1–4, 2014.

18. Hu, J., J. Huang, L. Kang, J. Zhou, Z. Zhang, and W. Peng, "Design of flexible broadband power divider based on defect ground compensation," *2020 IEEE MTT-S International Conference on Numerical Electromagnetic and Multiphysics Modeling and Optimization (NEMO)*, 1–4, 2020.

19. Heidari, S., R. Nemati, N. Masoumi, J. R. Mohassel, and N. Karimian, "DGS for a Wilkinson power divider using a symmetric butterfly comb," *2019 27th Iranian Conference on Electrical Engineering (ICEE)*, 264–268, 2019.

20. Chen, W., S. Li, Z. Wu, and Y. Liu, "Wideband power divider based on klopfenstein tapered line," *2019 International Conference on Microwave and Millimeter Wave Technology (ICMMT)*, 1–3, 2019.

21. Moradian, M., "Wideband in-phase slot-coupled power dividers," *AEU — International Journal of Electronics and Communications*, Vol. 82, 327–333, 2017.

22. Guo, L., H. Zhu, and A. Abbosh, "Wideband tunable in-phase power divider using three-line coupled structure," *IEEE Microwave and Wireless Components Letters*, Vol. 26, 404–406, 2016.

23. Younesiraad, H., M. Bemani, and M. Fozi, "A novel fully planar quad band Wilkinson power divider," *AEU — International Journal of Electronics and Communications*, Vol. 74, 75–82, 2017.

24. Liu, Y., S. Sun, and L. Zhu, "2^n-way wideband filtering power dividers with good isolation enhanced by a modified isolation network," *IEEE Transactions on Microwave Theory and Techniques*, Vol. 70, No. 6, 3177–3187, 2022.

25. Rahardi, R., M. Rizqi, W. D. Lukito, R. Virginio, M. Hilmi, and A. Munir, "Meander line-based Wilkinson power divider for unmanned aerial vehicle application," *2020 IEEE International Conference on Communication, Networks and Satellite (Comnetsat)*, 178–181, 2020.

26. Zhao, M., A. Kumar, C. Wang, B. Xie, T. Qiang, and K. K. Adhikari, "Design method of dual-band Wilkinson power divider with improved out-of-band rejection performance and high design flexibility," *AEU — International J. of Electronics and Communications*, Vol. 110, 152844, 2019.

27. Wong, S. W. and L. Zhu, "Ultra-wideband power divider with good in-band splitting and isolation performances," *IEEE Microwave and Wireless Components Letters*, Vol. 18, 518–520, 2008.

28. Ahmed, O. M. and A.-R. Sebak, "Experimental investigation of new ultra wideband in-phase and quadrature-phase power splitters," *Journal of Electromagnetic Waves and Applications*, Vol. 23, 2261–2270, 2009.

29. Osman, S. A. M., A. M. E. El-Tager, F. I. Abdelghany, and I. M. Hafez, "Two-way modified Wilkinson power divider for UWB applications using two sections of unequal electrical lengths," *Progress In Electromagnetics Research C*, Vol. 68, 221–233, 2016.

30. Chandrasekarani, S. S., S. R. Avaninathan, and P. Murugesan, "A meander coupled line wideband power divider with open stubs and DGS for mobile application," *Turkish Journal of Electrical Engineering* & *Computer Sciences*, Vol. 25, 3637–3644, 2017.

31. Hayati, M., A. Abdipour, and A. Abdipour, "A Wilkinson power divider with harmonic suppression and size reduction using high-low impedance resonator cells," *Radioengineering*, Vol. 24, 137–141, 2015.

32. Liu, W.-Q., F. Wei, C.-H. Pang, and X.-W. Shi, "Design of a compact ultra-wideband power divider," *2012 International Conference on Microwave and Millimeter Wave Technology (ICMMT)*, 1–3, 2012.

33. Ahmed, O. and A.-R. Sebak, "A modified Wilkinson power divider/combiner for ultrawideband communications," *2009 IEEE Antennas and Propagation Society International Symposium*, 1–4, 2009.

34. Zhou, B., H. Wang, and W.-X. Sheng, "A modified UWB Wilkinson power divider using delta stub," *Progress In Electromagnetics Research Letters*, Vol. 19, 49–55, 2010.

35. Liu, Y., L. Zhu, and S. Sun, "Proposal and design of a power divider with wideband power division and port-to-port isolation: A new topology," *IEEE Transactions on Microwave Theory and Techniques*, Vol. 68, 1431–1438, 2020.

36. Srisathit, K., P. Jadpum, and W. Surakampontorn, "Miniature Wilkinson divider and hybrid, coupler with harmonic suppression, using T-shaped transmission line," *2007 Asia-Pacific Microwave Conference*, 1–4, 2007.

37. Hazeri, A. R. and T. Faraji, "Miniaturisation and harmonic suppression of the branch-line hybrid coupler," *International Journal of Electronics*, Vol. 98, 1699–1710, 2011.

38. Weng, L. H., Y.-C. Guo, X.-W. Shi, and X.-Q. Chen, "An overview on defected ground structure," *Progress In Electromagnetics Research B*, Vol. 7, 173–189, 2008.

39. Lim, J.-S., Y.-T. Lee, C.-S. Kim, D. Ahn, and S. Nam, "A vertically periodic defected ground structure and its application in reducing the size of microwave circuits," *IEEE Microwave and Wireless Components Letters*, Vol. 12, 479–481, 2002.

40. Yu, T., "A broadband Wilkinson power divider based on the segmented structure," *IEEE Transactions on Microwave Theory and Techniques*, Vol. 66, 1902–1911, 2018.

41. Cohn, S. B., "A class of broadband three-port TEM-mode hybrids," *IEEE Transactions on Microwave Theory and Techniques*, Vol. 16, 110–116, 1968.

42. Steer, M., *Microwave and RF Design*, NC State University, 2019.

43. Nagi, H. S., "Miniature lumped element 180/spl deg/Wilkinson divider," *IEEE MTT-S International Microwave Symposium Digest, 2003*, Vol. 1, 55–58, 2003.

44. Ma, Z., W. Zhang, F. Liu, and M. Ohira, "A novel 10 MHz-4 GHz Wilkinson power divider using lumped compensation elements," *IEICE Electronics Express*, Vol. 19, 20210465, 2022.